Proceedings of the 11th ICPMG 2026
11th International Conference on Physical Modelling in Geotechnics
8-12 June 2026, Zurich, Switzerland

Experiments on reinforced earth dams in full scale

M. Tillmanns
Karlsruhe Institute of Technology (KIT), Karlsruhe, Germany, maximilian.tillmanns@kit.edu

J. Rabold
Karlsruhe Institute of Technology (KIT), Karlsruhe, Germany, jan.rabold@kit.edu

A. Bieberstein
Karlsruhe Institute of Technology (KIT), Karlsruhe, Germany, andreas.bieberstein@kit.edu

S. Schiller
Bermüller & Co. GmbH, Nuremberg, Germany, sebastian.schiller@beco-bermueller.de

C. Harmening
Karlsruhe Institute of Technology (KIT), Karlsruhe, Germany, corinna.harmening@kit.edu

H. H. Stutz
Karlsruhe Institute of Technology (KIT), Karlsruhe, Germany, hans.stutz@kit.edu

ABSTRACT: The large amount of area required for conventional flood protection structures, such as embankment dams and levees, often leads to conflicts with property owners. These disagreements result in lengthy planning and approval procedures, which take time that is not available in view of the increasing risk of flood events. This turns area into a resource, which is becoming increasingly important in the flood protection of the future. Obviously, flood protection systems with reduced area requirements would make a contribution to accelerated and modern flood protection. Dams of reinforced earth could offer a possibility to overcome this issue. For this reason, experiments on reinforced dam models with slopes of 70 degrees are carried out, with the aim to investigate the possibility of building resource-saving earth dams that meet the requirements of the applicable regulations. The experiments are performed on dam models with crest heights of 2.25 meters, which are equipped with different measurement technologies. The seepage water flow is recorded. Deformations of the dam surface during different loads are measured using a terrestrial laser scanner. Tensiometer water sensors determine the seepage line inside the dam. Initial results show that space savings of more than 70% are potentially possible. In the experiment no considerable deformations or displacements were determined. Even the seepage water in the most critical case of sealing failure appears to be manageable because the drain can be adequately dimensioned and the sealing system used is capable of sealing small damages itself.

1 INTRODUCTION

Floods have always been a part of the natural water cycle. Although humanity has repeatedly experienced the associated threats, 1.8 billion people still live in areas at risk of flooding (Rentschler et al., 2022). A key part of the problem lies in settlements located near rivers, which regularly lead to land-use conflicts in the context of flood protection. The large space requirements, particularly for dam-like flood protection structures designed according to DIN 19700 respectively DIN 19712, and the associated compensatory measures result in planning, approval, and implementation periods that require a significant amount of time. Time that, in light of increasing flood risks, is not available.

To address this issue, flood protection structures with reduced space requirements could make an important contribution. Since cost-effective earth construction is to be maintained and the concept of resilience is gaining increasing importance, the question arises as to whether it is possible to construct earth dams that are permanently stable, safe, and functional while requiring significantly less space.

For this aim it is investigated whether reinforced earth structures can serve as a safe alternative for flood protection facilities in areas with limited space. The goal of the investigation is to ensure the safe construction of earthen dams with up to three times smaller base widths. This paper presents setup, performance, and first results of full scale experiments on reinforced earth dams.

2 FLOOD PROTECTION DAMS CONSTRUCTED WITH REINFORCED EARTH TECHNIQUES

Dams constructed with reinforced earth techniques are primarily known in civil engineering from infrastructure projects, such as roadway embankments or (noise) protection barriers designed according to EBGEO. However, the use of reinforced earth for the construction of slender dam structures subjected to hydraulic loads represents an entirely new application. To demonstrate the required reliability, this construction method must be thoroughly investigated.

The investigations are being carried out on physical dam models at various scales. Initial exploratory tests were conducted on a laboratory scale of 1:5 (Tillmanns et al., 2025). After the laboratory experiments, experimental dams in full scale were analysed.

To identify a suitable space-efficient dam system, a preliminary selection of dam cross-sections was made. Based on various criteria, this selection was narrowed down to a single preferred cross-section for the presented experiments. This preferred cross-section features a three-zone dam incorporating a geosynthetic clay liner (GCL) as an impermeable barrier and a toe drain (see Figure 1). The slope inclination of 70 degrees results from the chosen reinforced earth system. This system consists of a polymeric-coated hexagonal steel wire mesh, laid in overlapping layers, with a mesh size of 8 × 10 cm and a wire diameter of 3.2 mm. The uniformity of the slope face is ensured by a steel mesh panel serving as a lost formwork.

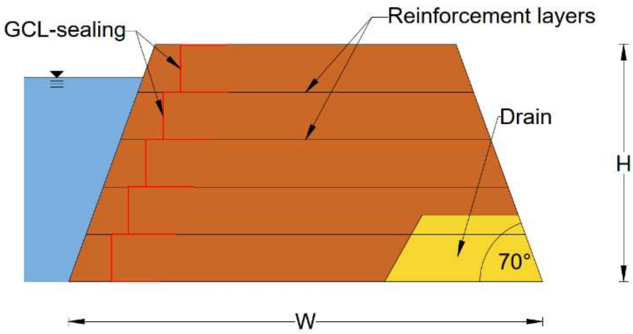

Figure 1. Preferred dam cross-section consisting of five reinforcement layers.

As a characteristic parameter of the dam geometry, a height-to-width ratio (H:W ratio) has proven effective so far. In this ratio, the dam crest height is related to the base width (see Figure 1). This provides a scale- and height-independent measure of the base width, which is decisive for determining the required space. The laboratory experiments reportet by (Tillmanns et al., 2025) suggest that an H:W ratio of 1:2 can provide satisfactory results if only the dam is taken into account.

The focus of the current investigations is on initial deformation analyses and the determination of the geohydraulic behavior of dams at a technical scale under various hydraulic loading conditions. In the experiments presented here, the dam and its foundation were not considered as a combined system, although such an integrated approach is essential for the design of these structures.

In addition to assessing whether the sealing system used meets the specified requirements, the question also arises as to how the seal behaves in the event of damage. Preliminary studies suggest that the bentonite contained within the system may be able to reseal small holes in the liner through swelling. The experiments presented here were intended to investigate whether this self-healing effect also occurs in geosynthetic clay liners used in dams.

3 PHYSICAL DAM MODEL

3.1 Experimental objective

The purpose of the performed experiments was to gain more information about the possible realization of reinforced earth dams for flood protection. Due to the definition of reliability, consisting of stability, durability, and serviceability, in particular the determination of the flow-through conditions and the measurement of dam surface deformations were the focus of the investigations. Therefore, different states of hydraulic loading were applied and the reaction of the dam was monitored.

The behavior of the sealing in the event of possible damage was also investigated. For this purpose, the sealing was perforated at specific points with the aim of quantitatively recording the reaction of the sealing system and the structure.

A special interest in testing was the tightness of the sealing system. For this reason, the seepage water was measured as well.

3.2 Experimental reinforced dam

The test dam was constructed on a scale of 1:1 from three layers of reinforcement, each 75 cm thick (see Figure 2). This resulted in a total height of 2.25

m. Based on laboratory tests, an H:W ratio of 1:2 was selected, resulting in a dam width of 4.5 m.

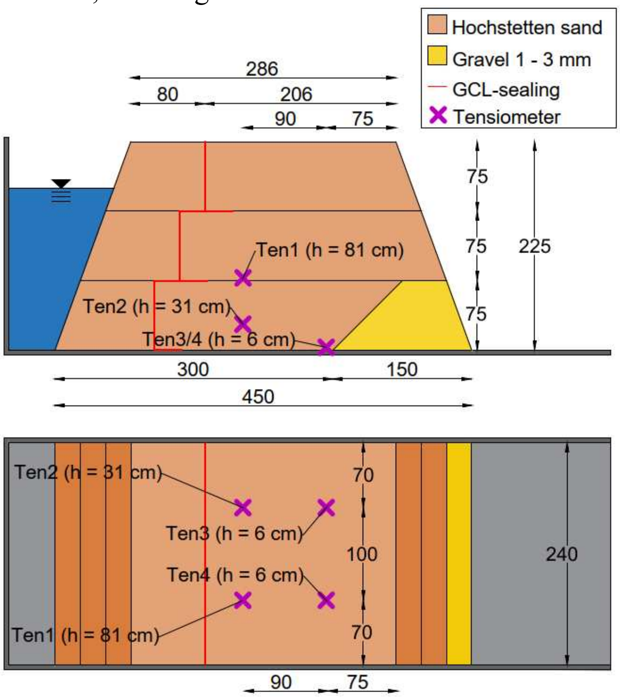

Figure 2. Dimensions of the test dam, positions of tensiometers and their height above ground h in cm (above: side view, below: top view).

A steel container open on one side with dimensions L x H x W = 6.5 x 2.3 x 2.4 m was used as a water tight test setup (see Figure 3). The dam was installed in the container so that the downstream side of the dam corresponded to the open side of the container and the closed side could form a water basin. The dam length was thus set at 2.4 m. This experimental setup has already been used successfully several times in (Riegger, 2013) for dam tests.

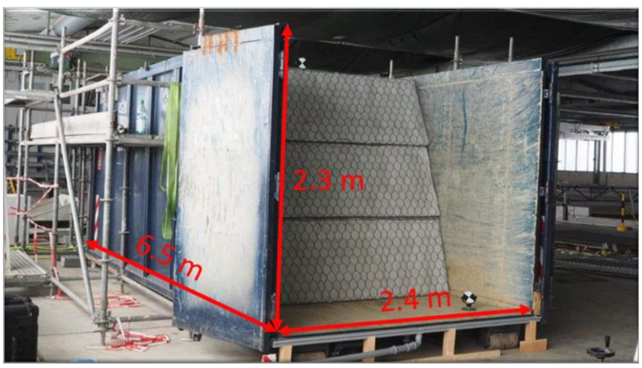

Figure 3. Container as test setup with dimensions and reinforced test dam.

So-called “Hochstetten sand” was used to construct the test dam. This is a naturally occurring sand with a cohesion of 16.8 kN/m², a friction angle of 38.6° and a permeability of $2 \cdot 10^{-4}$ m/s. The grain size distribution of “Hochstetten sand” is shown in Figure 4. This sand has been used because it will be used later in upscaled experiments.

The dam was constructed using a GCL described in Section 2. The GCL-sealing was created from three sub-elements, corresponding to the reinforcement layers. At the sealing joints, the GCL was laid parallel to the reinforcement over a length of 30 cm and the resulting gap was filled with bentonite granulate to create an appropriate seal.

The reinforcement layers were installed through the whole cross-section. The slope elements are anchored to the top and bottom of the retaining structure by continuous reinforcement. To prevent the embankments from bulging, a structural steel mesh without a static function is installed on the front sides. As part of the test, no vegetation was allowed to grow on the slope and erosion protection was ensured by a geotextile. This enables more precise measurement of the dam contour.

The length of the bottom drain was chosen to be one third of the dam width and was therefore 1.5 m. The upstream side of the drain was constructed at an angle of 45°. Gravel 1-3 mm was used as the material for the bottom drain (see Figure 4).
The Hochstetten sand was dynamically compacted to 95–97% of the previously determined Proctor density.

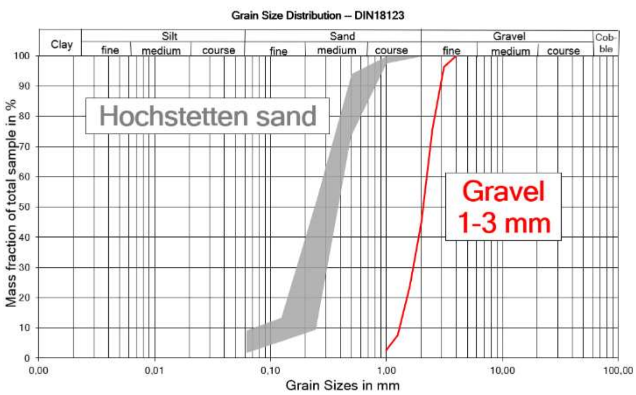

Figure 4. Grain size distribution of Hochstetten sand and Gravel 1-3 mm.

3.3 Measurement and monitoring technology

3.3.1 Deformation measurements using TLS

Terrestrial Laser Scanning (TLS) is a highly precise, non-contact technique for the three-dimensional acquisition of object surfaces. Terrestrial laser scanners operate as polar measurement instruments, based on the recording of two spatial angles in combination with a time-synchronized distance measurement. In addition to the range measurement, an intensity value representing the backscattered energy is derived (Schwarz, 2018).

The Imager 5016's range noise ranges between 0,3 mm and 0,5 mm (Zoller+Fröhlich, 2024). By deflecting the measurement beam using high-frequency rotating mirrors, scan rates of up to one million points per second can be achieved (Schwarz, 2018). The acquired data are stored as point clouds, representing discrete three-dimensional samples of the scanned surfaces.

Figure 5. Zoller + Fröhlich Imager 5016 positioned on the upstream side (left) and on the downstream side (right).

The recorded point clouds constitute position-dependent subsets of a scene or temporal snapshots acquired at specific moments in time (so-called epochs). Through registration, these independent point clouds are spatially aligned and transformed into a common coordinate system. In TLS applications, target-based registration using dedicated reference markers has become the standard approach (Schwarz, 2018). Registration is typically performed using at least three homologous points and a seven-parameter transformation (Niemeier, 2008). Algorithms such as the Iterative Closest Point (ICP) method iteratively minimizes point-to-point distances between overlapping datasets (Besl & McKay, 1992; CloudCompare, 2024). Registration of the downstream side point clouds was solely based on reference markers resulting in a residual error of 0,7 mm. The upstream side point clouds were registered using reference markers and ICP resulting in a residual error of 0,6 mm.

For the quantitative analysis of surface changes between different epochs, the M3C2 algorithm (Multiscale Model to Model Cloud Comparison) has emerged as a standard method (Lague et al., 2013). This approach allows direct distance computation between two point clouds along local surface normals, while explicitly accounting for local surface geometry and point density. As a result, morphological changes — for example, those induced by erosion, deformation, or construction processes — can be quantified with high precision and low noise, without the need for prior gridding or surface approximation.

As part of the experiments presented here, the terrestrial laser scanner was positioned on both, the upstream and the downstream sides (see Figure 5), and the dam structure was surveyed after each loading condition. This enabled a deformation analysis of the slopes on the upstream and downstream sides, respectively. On the upstream side, it was not possible to survey the entire slope due to limitations of the scanner. A circular area at the lower part of the slope could not be scanned. The deformations were determined using the previously described M3C2 algorithm. Surveying the crest with the laser scanner proved challenging, as the incidence angle of the laser beam was too shallow and the reflections therefore did not provide reliable results. Consequently, five flat targets were arranged (see Figure 6) and their settlement compared to the initial state was evaluated using the software provided by Zoller + Fröhlich.

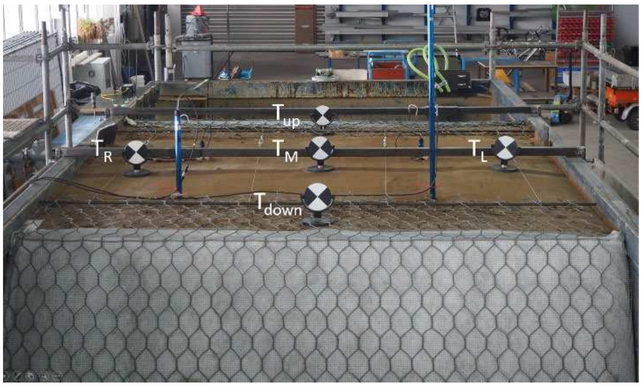

Figure 6. View on target arrangement from downstream side.

3.3.2 Seepage

To determine the flow through the dam, the pore water pressure in the dam body was measured at four points and the amount of seepage was measured. The tensiometers used to measure the pore water pressure were calibrated shortly before installation and subsequently installed in two cross-sections in the dam body. Their positioning is shown in Figure 2. Data acquisition using the tensiometers was ensured on a continuous basis.

The seepage escaping from the dam was measured manually at individual points in time. The magnetically induced flow meter installed for continuous data acquisition was unable to detect the low flow rates.

3.4 Load Conditions

Only hydrostatic loads acted on the dam structure. Different water levels, impoundment durations, and different drawdown rates were used for this purpose. Other loads, such as traffic loads, were not taken into account in these tests.

The simulated conditions were derived from the regulations applicable in Germany. In particular, the requirements of DIN 19700 “Dam Structures” and DIN 19712 “Flood Protection Structures on Watercourses” were taken into account.

This resulted in the following load situations:

1. Design flood level
2. Crest impoundment
3. Rapid drawdown
4. Perforated sealing

The design flood level was set at 1.75 m. This corresponds to a freeboard of 0.5 m, which is the minimum freeboard according to DIN 19700. The impoundment took place in stages, first in two 0.5 m steps, then in three 0.25 m steps. There was a two-hour pause between each step. At a water level of 1.0 m, the water level was kept constant for 12 h. Once the design flood level of 1.75 m had been reached, the water level was maintained for three days. This was followed by a slow drawdown at 5 cm/h.

The crest impoundment was set at 5 cm below the dam crest. The water level in the crest impoundment load case was thus 2.20 m. The reservoir was again filled in stages. The first 1.5 m were raised in two steps of 75 cm each, and the remaining 75 cm were filled in three steps of 25 cm each. The impoundment interruptions lasted two hours each. At a water level of 1.5 m, the water level was kept constant for 18 h. After completion of the impoundment, the water level was kept constant for 30 h. The drawdown was carried out at a medium speed with a sinking rate of 10 cm/h.

The third stress situation involved a rapid drawdown. For this purpose, the dam was filled in two equal stages to 1.75 m (corresponding to the design flood level). After the water level had been kept constant for 20 h, the reservoir was emptied very quickly. The lowering time was 66 min until complete emptying. This corresponds to a lowering speed of approx. 160 cm/h.

For the final loading scenario, the sealing system was intentionally damaged. For this purpose, the GCL was to be uniformly perforated at 25 locations over the entire hydraulically loaded height. The sealing of the existing dam was pierced using a steel rod with a diameter of 22 mm (see Figure 7). After the experiment was completed, it was found that the sealing had actually been punctured at 23 locations. Subsequently, the dam was impounded up to the design flood level, and the response of the dam and the sealing system was examined. The test was continued until steady-state conditions were reached. The drawdown was carried out with an undefined sinking rate.

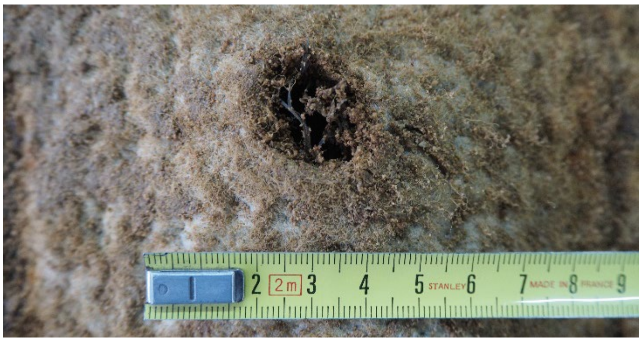

Figure 7. Artificially introduced hole in the GCL-sealing.

4 EXPERIMENTAL RESULTS

4.1 Deformations

Two point clouds generated from the terrestrial scans are shown as examples in Figure 8.

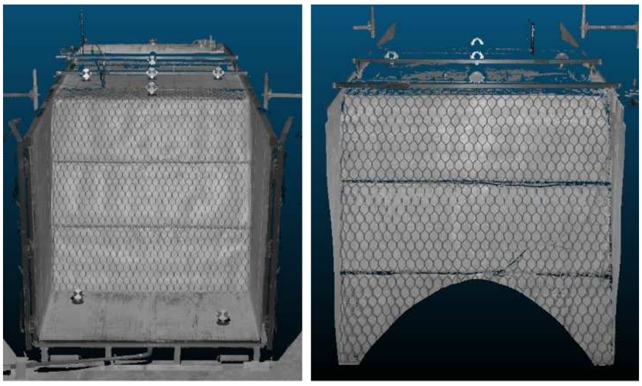

Figure 8. Representative point cloud of downstream side (left) and upstream side (right). The greyscale values indicate the backscattered intensity.

By comparing the point clouds from the scans before and after each loading scenario, deformations normal to the dam surface were identified.

The results obtained for the upstream side are shown in Figure 9 a – d. Although the magnitudes of the M3C2 distances are comparable with those of the downstream side, systematic patterns can be seen in Figure 10 a and b, indicating small deformations in the range of several millimeters. These can be attributed to massive erosion effects at the edges, which occurred during the first two loading scenarios (design flood and crest impoundment). During the second loading scenario, the erosion extended up to the crest surface (see Figure 11).

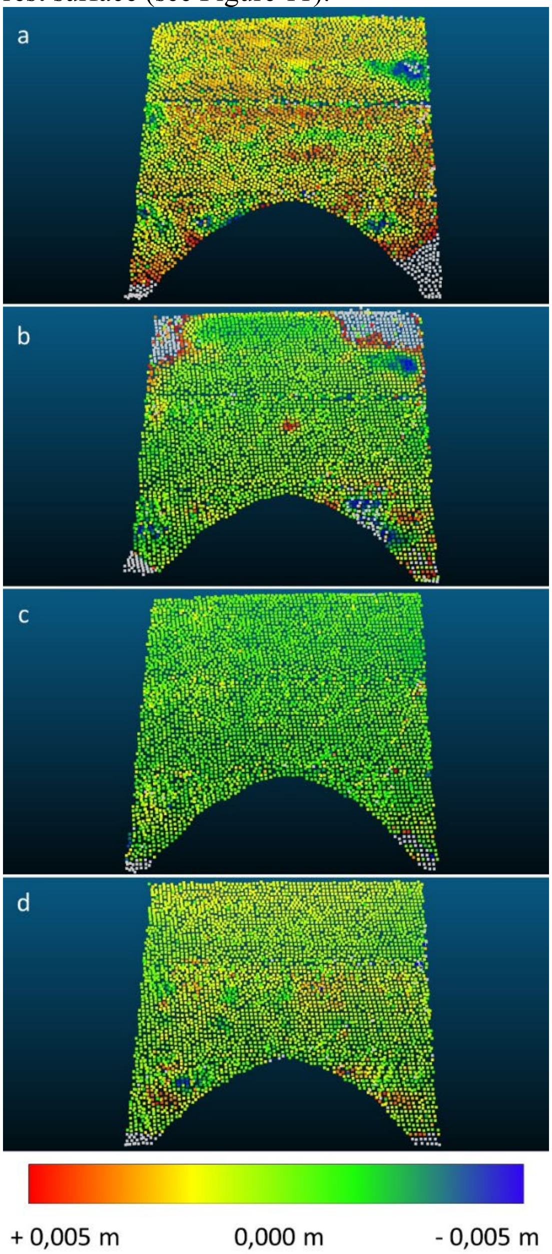

Figure 9. Results of the M3C2 deformation analysis of the upstream slope for a) design flood, b) crest impoundment, c) rapid drawdown, and d) damaged sealing, with legend of normal deformation in meters.

The deformations of the downstream side slope in terms of the M3C2 distances for all loading conditions are shown in Figure 12 a–d. It can be observed that the point clouds differ by a maximum of 3 to 5 mm with no systematic deformation patterns being visible. Therefore, the differences are assumed to arise solely due to measurement uncertainties and can be evaluated as not considerable.

The conclusion that only small deformations can be detected can also be applied to the settlement measurements of the dam crest. The vertical displacements determined for the loading scenarios design flood level, crest impoundment, and damaged sealing, as well as a comparison between the first and last measurement, are presented in Table 1. Although the magnitude of the coordinate differences is small, the systematic behaviour of the five targets indicate a settlement of the crest about few millimeters, especially in the last two load cases.

Table 1. Measured settlements (negative) and heavings (positive) of the flat targets on the dam crest for the design flood level, crest impoundment, and damaged sealing, expressed in millimetres.

	Design level	**Crest impoundment**	**Damaged sealing**
T_{down}	1	-7	0
T_L	2	-1	-1
T_M	1	-2	-1
T_R	1	-2	-1
T_{up}	2	-2	0

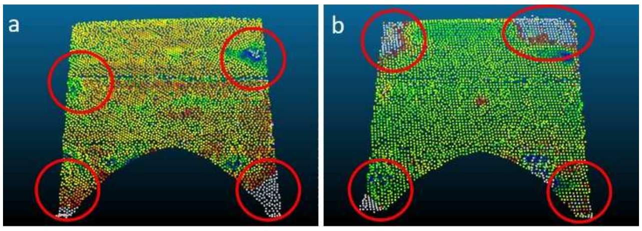

Figure 10. Result of the M3C2 analysis of the upstream side, with markings for deformation caused by erosion due to boundary processes for a) design flood and b) crest impoundment.

Figure 11. Visible erosion processes on the dam surface.

4.2 Seepage

During the loading scenarios representing the design flood, crest impoundment, and the rapid drawdown, no measurable seepage through the dam could be detected. The sealing system used remained impermeable under the applied hydraulic loads.

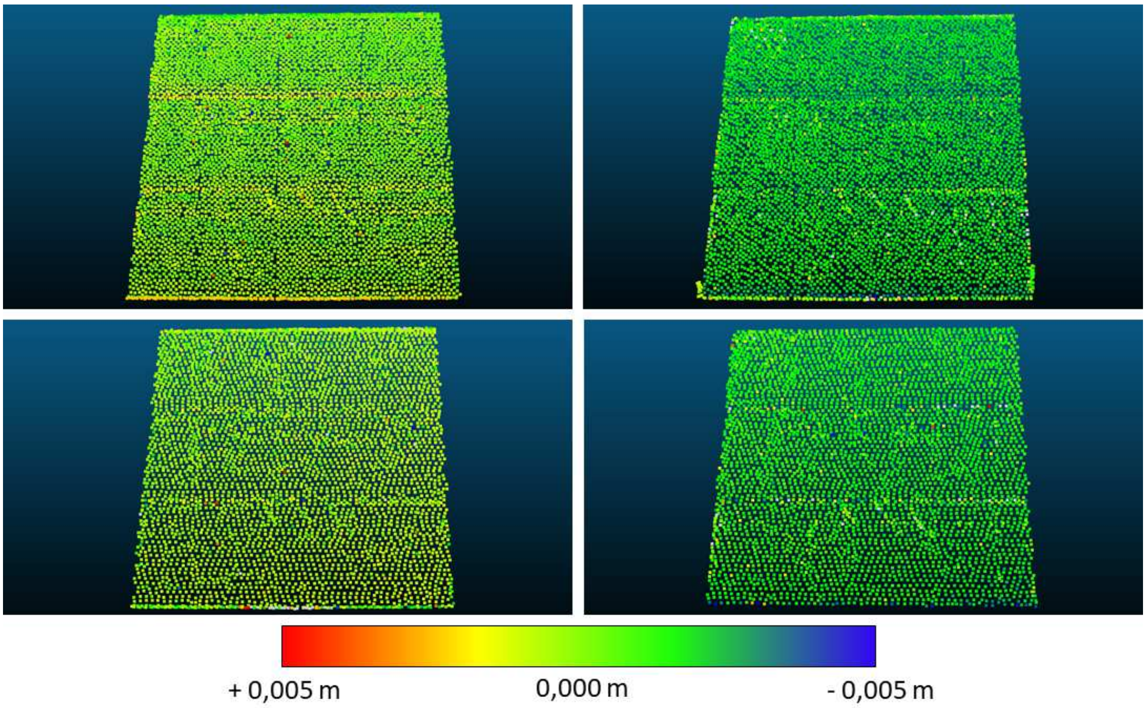

Figure 12. Results of the M3C2 deformation analysis of the downstream slope for a) design flood, b) crest impoundment, c) rapid drawdown, and d) damaged sealing, with e) legend of normal deformation in meters.

In the experiment in which the GCL was perforated, measurable seepage through the dam was observed. As shown in Figure 13, a flow rate of 0.99 ml/s per meter dam length was recorded after approximately 21 h. This flow rate gradually decreased with time, until steady-state conditions were reached after about 19 days (456 h). In the steady state, the flow rate amounted to 0.13 ml/s/m.

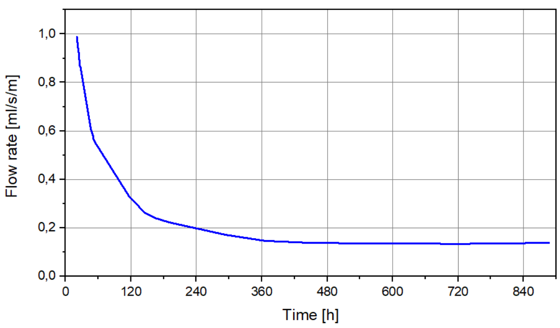

Figure 13. Flow rate over time for perforated sealing experiment.

This observation was also supported by the tensiometer measurements. As illustrated in Figure 14 all tensiometer readings show a peak after approximately 15 h. Due to several measurement failures (indicated as dashed lines in Figure 14), the pore water pressure development could not be completely recorded. Nevertheless, it can be observed that the trend of the measured pore water pressures correspond well to the flow measurements. The maximum values u_{max} and steady-state values u_{steady} after 150 h of the tensiometer readings are summarized in Table 2, except for the steady steady-state value of tensiometer Ten2, which could not be determined.

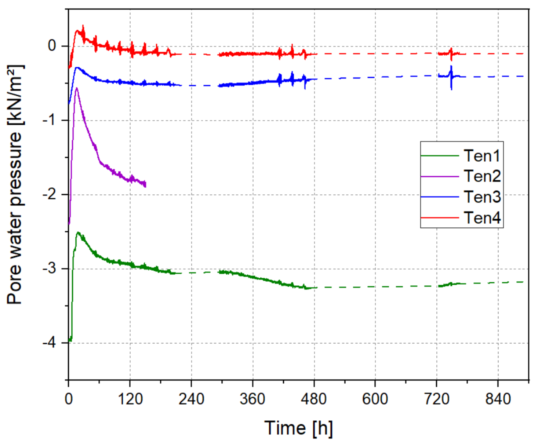

Figure 14. Tensiometer readings, measurement failures as dashed lines.

Before conducting the experiment, it was assumed that the bentonite contained in the geosynthetic clay liner might close the artificially introduced holes due to its swelling properties. The decreasing trends of both, the flow and tensiometer measurements support this assumption. Furthermore, the geosynthetic clay liner was examined after dismantling. It was found that 22 of the 23 perforation holes had indeed resealed as expected (see Figure 15). Since the perforation tool was lost within the liner at one location during installation, it could only be confirmed at one position that no self-healing effect occurred.

Table 2.Maximum and steady-state tensiometer values in kN/m².

	Ten1	Ten2	Ten3	Ten4
u_{max}	-2.53	-0.6	-0.29	-0.21
u_{steady}	-3.02	-	-0.5	-0.09

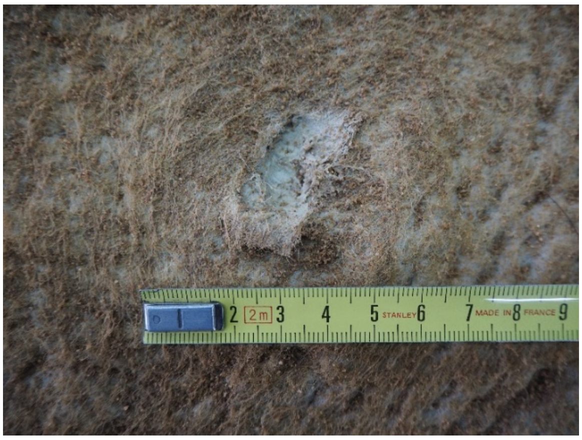

Figure 15. Self-healing of the sealing due to the swelling of bentonite.

5 CONCLUSIONS

Within the scope of the experiments presented here, it was found that the deformations of the dam structure were on the order of millimetres and thus tolerable. Larger deformations occurred only locally and could be attributed to boundary effects. The hydraulic investigations showed that the sealing system used is almost watertight under the given conditions. After the sealing was manually damaged, a self-healing effect could be observed based on flow and pore water pressure measurements, which can be attributed to the bentonite contained in the GCL. This hypothesis was later confirmed through analysis of the sealing. Upon completion of the experiments, it can be concluded that the dam structure meets the specified hydraulic and structural requirements under the given conditions. Further investigations are now necessary to determine the limitations of these findings. In addition, questions regarding erosion safety, subsoil hydraulics, durability and quality assurance will guide future research.

ACKNOWLEDGEMENTS

The authors gratefully acknowledge the financial support of this work by the ZIM (Zentrales Innovationsprogramm Mittelstand, KK5633401MN3) program and the Federal Waterways Engineering and Research Institute (BAW) for providing the opportunity to conduct the experiments at their facilities.

REFERENCES

Besl, P. J. & Neil D. McKay (1992). A Method for Registration of 3-D Shapes. *IEEE Transactions on pattern Analysis and Machine Intelligence*. Vol. 14. No.2

CloudCompare (2024). *3D Point Cloud and Mesh Processing Software. Online*. Available at: https://www.cloudcompare.org

DIN 19700 - *Stauanlagen. Dam plants. Standard*. DIN e.V. (in German).

DIN 19712 - Hochwasserschutzanlagen an Fließgewässern. *Flood protection works on rivers. Standard*. DIN e.V. (in German).

EBGEO - Empfehlungen für den Entwurf und die Berechnung von Erdkörpern mit Bewehrungen aus Geokunststoffen. *Recommendations for the design and calculation of earth structures with geosynthetic reinforcement*. Deutsche Gesellschaft für Geotechnik e.V. Berlin: Ernst (in German).

Hazen, A. (1911). Discussion of "Dams on Sand Foundations" by A. C. Koenig. *Transactions of the American Society of Civil Engineers*, 73, 199–203.

Lague, D. et al. (2013). Accurate 3D comparison of complex topography with terrestrial laser scanner: Application to the Rangitikei canyon (N-Z). In: *ISPRS Journal of Photogrammetry and Remote Sensing* 82: 10–26.

Niemeier, W. (2008). *Ausgleichungsrechnung: statistische Auswertemethoden. Adjustment computation: statistical evaluation methods*. 2nd edition. De Gruyter Textbook. Berlin, New York: Walter de Gruyter (in German).

Rentschler, J., Salhab, M. & Jafino, B.A. (2022). Flood exposure and poverty in 188 countries. *Nat Commun* 13, 3527. https://doi.org/10.1038/s41467-022-30727-4.

Riegger, T. (2013). *Sicherung quasihomogener Altdeiche mittels Dränelementen. Securing quasi-homogeneous old dikes using drainage elements*. Karlsruhe Institute of Technology (KIT) (in German).

Schwarz, W., Hrsg. (2018). Ingenieurgeodäsie: Handbuch der Geodäsie. *Engineering Geodesy: Handbook of Geodesy*. Berlin, Heidelberg: Springer (in German).

Tillmanns, M., et al.. (2025). Development of space-efficient dam structures for technical flood protection. In *Proceedings of the 5th Fachsektionstage Geotechnik – Interdisziplinäres Forum*, Würzburg, Germany, October 7–8 (pp. 571–576). Karlsruhe Institute of Technology. ISBN 978-3-946039-13-6. (in German).

Zoller+Fröhlich (2024). *Z+F IMAGER 5016|5016A|Z+F FlexScan 22*. Technical Datasheet.